Open Ceramics 16 (2023) 100492

Contents lists available at ScienceDirect

Open Ceramics

journal homepage: www.sciencedirect.com/journal/open-ceramics

Spray drying as a one-step production method of SiC-based granulates for direct reactive laser sintering of Reaction Bonded Silicon Carbide (RBSiC)

Jan Huebner [a,b,*], Stefan Pfeiffer [b], Paweł Rutkowski [a], Łukasz Wójcik [a], Dariusz Kata [a], Thomas Graule [b]

[a] AGH University of Science and Technology, Faculty of Material Science and Ceramics, Kraków, Poland
[b] EMPA, Swiss Federal Laboratories for Materials Science and Technology, Laboratory for High Performance Ceramics, Dübendorf, Switzerland

ARTICLE INFO

Handling Editor: Dr P Colombo

Keywords:
Reaction bonded silicon carbide
Spray drying
Laser processing
Granulation
Powder characterization

ABSTRACT

This research is focused on the development and production of SiC-based granulates for reactive laser sintering. Ceramic slurries with different compositions of SiC, Si, C powders, and PVA binder were subjected to spray drying. Carbon source in form of latex was proposed to avoid a reaction of Si with H_2O in alkalic pH caused by the presence of carbon in the slurry. It was observed that the latex was beneficial for improvement of the flowability. Selected granulates were subjected to laser processing using two different methods. The first one where SiC-based granulates were spray deposited on a SiC substrate and laser treated with single pulse working of the laser. The second method where a pressed green sample of SiC were processed by the continuous working mode of the laser. Results revealed that the use of the continuous work mode during laser processing allowed to produce Reaction Sintered SiC (RBSiC).

1. Introduction

Conventional sintering of pure SiC is generally time-and energy-consuming. The shaping freedom is limited by the conventional sintering techniques (hot pressing, pressureless sintering, recrystallization sintering, microwave sintering [1]) as well as post-machining, due to the high hardness and wear resistance of SiC [2]. Direct reactive laser sintering of Reaction Bonded SiC (RBSiC) by the use of SiC-based granulates with Si and C addition for sintering can be a new way to solve these problems. It can be further modified in order to use 3D imaging to develop additive manufacturing method of RBSiC sintering, which will allow for far greater shape freedom of the finished product [3]. Silicon carbide is a suitable material for laser processing due to its material properties such as high thermal shock resistance, high-temperature stability, low coefficient of thermal expansion, high thermal conductivity, and high light absorptivity in the visible and near-infrared range [2]. This allows to withstand extreme temperatures that are induced locally by high powered laser beam.

Ceramic materials are typically manufactured by bottom-up methods, which are defined as processes that use powder-based materials to firstly prepare a desired shape and then are followed by sintering. This leads to limitations in terms of possible geometry of the final product. Because of high temperatures needed for ceramics to form a liquid phase and increase the diffusion rate, reactive sintering aids (Si, SiO_2, B, B_4C, Al, Be) [1] can be introduced to the systems for sinterability enhancement. In case of laser techniques such as Selective Laser sintering (SLS), the reactants are generally prepared as a powder or granulate. During processing, the powder is subjected to a high-power laser beam which allows for local consolidation of materials.

Silicon carbide (SiC) and Silicon Nitride (Si_3N_4) are considered suitable to be used as both: porous materials and dense elements for structural applications. The advanced ceramic SiC is characterized by a combination of specific properties such as low density, high thermal conductivity, high melting point ($T_m = 2600$ °C [4]), excellent ablation and wear resistance, high strength at both room and elevated temperatures, high thermal and chemical stability, excellent corrosion resistance and low thermal expansion coefficient [2]. This makes it suitable for its application in high temperature environments. The idea of reactive sintering of SiC is widely known [5–11]. Due to multi-stage processing, overall complexity, and limitations in obtainable shapes, most of these production methods are limited for applications requiring a high density of the material such as thermal shielding, electromagnetic wave shielding, high performance brake systems; and highly porous materials e.g. filters for air pollution, wastewater, molten metal, and exhaust

* Corresponding author. AGH University of Science and Technology, Faculty of Material Science and Ceramics, Kraków, Poland.
E-mail address: huebnerj@agh.edu.pl (J. Huebner).

https://doi.org/10.1016/j.oceram.2023.100492
Received 25 July 2023; Received in revised form 27 September 2023; Accepted 14 October 2023
Available online 16 October 2023

gases. SLS can be a solution that would allow the manufacturing of parts with advanced geometry.

Different SiC production methods were already developed, which can be divided into two groups. The first one is focused on obtaining materials with high density:

- Reaction bonded SiC (RBSiC) with different sintering aids, able to obtain high relative density [12,13].
- Molten silicon infiltration of C/SiC preform, which allows fabrication of dense reaction bonded Si/SiC [14].
- Pyrolysis of ferrocene-modified polycarbosilane (PCS) mixed with inert filler Si_3N_4 powders followed by heat treatment up to 1400 °C which led to dense structure [15].
- Hot-pressed SiC/Si_3N_4 doped by AlF_3 and MgF_2 with high density, high thermal conductivity, and enhanced mechanical properties [5].
- SiC reinforced by Si_3N_4 whiskers prepared by in situ reaction of SiC/Si with N_2 in order to produce SiC/Si_3N_4 composite. The uniform distribution of Si_3N_4 whiskers throughout the volume of a sample provided a high density of material [9].
- Laser-induced gas phase reaction synthesis of SiC/Si_3N_4 dense composite [8].

The second group consists of processes suitable for the manufacturing of highly porous structures that keep a relatively high strength of SiC-based ceramics as shown below:

- Porous SiC/Si_3N_4 obtained by freeze casting followed by carbothermal reduction reaction [7].
- Porous SiC/Si_3N_4 ceramics obtained by chemical vapor infiltration and reaction which used paper preforms [11].
- Highly porous SiC/Si_3N_4 obtained by reaction sintering method with the addition of Y_2O_3 as sintering aid [10].
- Protein-based gel casting followed by a modified SPS method in order to produce highly porous (60–70%) SiC/Si_3N_4 foams [16].

The shaping limitations of the traditional processing methods can be solved by the application of additive manufacturing (AM) methods such as selective laser sintering (SLS) [12] or others including slip casting, freeze casting, or gel casting followed by sintering process [6,7,16]. The SLS method is still in a development stage in the field of ceramic materials. It uses powder reactants that are sintered by laser beam and offers the possibility to manufacture geometrically complex parts. This grants the possibility to modify and adjust the process in order to obtain the desired final properties such as controllable porosity, gradient structures and high dimensional accuracy by a small spot size.

The powders needed for successful SLS processing of SiC-based ceramics need to meet specific requirements. One parameter used widely to describe the quality of powders is flowability. It gives information about the significance of inter-particle forces in powders subjected to free fall [17]. It can be described by various parameters. The most used one is the Hausner ratio, which is defined as the relation between tapped density (d_{tap}) and apparent density of the powder (d_{app}) [17]:

$$H = \rho_{tap}/\rho_{app}$$

Table 1
Hausner ratio.

Hausner Ratio	Flow character
1.00–1.11	Excellent
1.12–1.18	Good
1.19–1.25	Fair
1.26–1.34	Passable
1.35–1.45	Poor
1.46–1.59	Very poor
>1.60	Bad

It is useful as it reflects particle-to-particle friction [18]. The closer the value is to 1, the better flowability of the tested powder as seen in Table 1. Values considered to be good enough for SLS, range from 1.00 to 1.25 [19].

Because SiC powders are characterized by a rough particle shape, which lowers the flowability, it is necessary to develop a new preparation route that allows to obtain spherical granulates that are suitable for SLS. Additionally, in order to improve the sinterability of such material, the introduction of various sintering aids is necessary.

Previously conducted studies used commercially prepared SiC granulates/powders that were further mixed, by mechanical methods, with sintering additives. On the contrary, the approach proposed in this study is based on a modification of the initial granulate composition. It was possible through careful analysis and optimization of the spray drying process which starts with the preparation of ceramic slurry. This allowed to obtain granulates with designed compound content (SiC, Si, and C with a very small addition of binding agent in the form of PVA or latex particles). As a result, manufactured powders are characterized by spherical shape (especially granulates with latex) which is translated to great flowability properties necessary for the SLS process. Because of the one-step nature of the spray drying process, it resulted in a very homogenous distribution of different compounds throughout every single granule which ensures uniform microstructural properties after SLS.

The novelty presented in this research is a one-step production method with high control of final granulate properties in comparison to previously used methods employing the mixing of commercially available powders with sintering aids. The SLS proved to be successful in producing dense SiC-based materials. The addition of fine Si particles have two main purposes. Firstly, it enables formation of a liquid phase necessary for consolidation because of its low melting point MP_{Si} = 1414 °C. Si also can react with carbon, either introduced separately to the system or originating from organic binders in the granulate. The spray drying method was previously proved as suitable for production of oxide powders for laser manufacturing [20–23].

2. Material and methods

2.1. Spray drying of granulates

Commercially available powders of SiC F2000 (SIKA Fiven, Norway), Si 1–5 μm (Atlantic Engineer Equipment, USA), Si 0.5 μm (US Research Nanomaterials, USA), and C PAK1000 (Rütgers CarboTech GmbH, Germany) were used for ceramic slurry preparation. In order to prepare the slurry PVA addition (M_W = 31000 ÷ 50000 g/mol, 99%, Sigma Aldrich, USA) was used as a binder. Latex polystyrene 50 wt% water suspension (Trinseo, USA) of spherical shape (d = 450 nm) was used for preparation of selected granulates as an alternative carbon source. Slightly acidic pH of about 5.5–7.0 was controlled by adding HCl or NH_4OH (0.01 mol water solution) in the appropriate amount. The preparation of SiC-based granulates by spray drying was conducted using a Büchi Mini Spray Dryer B-290 (Büchi Labortechnik, Switzerland). Spray drying was performed with a two-fluid nozzle in co-current mode.

2.2. Selective laser sintering

Laser sintering was conducted on a prepared surface in an isolated reaction chamber (JK Laser 5000, JK Laser, UK). It is equipped with Nd:YAG fiber laser with a wavelength of 1064 nm, which is suitable for SiC processing (absorptivity of this wavelength by SiC ≈ 78% [24]). Spray deposition employing airbrush (Patriot-105, Badger, USA) was used for consequent layer deposition. This no-contact method uses alcohol or water-based dispersions for the deposition of thin layers, which prevents accidental destruction of granules before sintering. Nitrogen was used as a shielding gas in order to prevent oxidation. Additionally, some of the granulates were pressed into green samples and subjected to laser

processing with the same parameters in order to investigate sintering of a single SiC layer.

2.3. Granulate and sample analysis

Initial powders and obtained granulates were characterized by means of SEM (Tescan VEGA3, Tescan Instruments, Czech Republic), helium density (Ultrapyc 5000, Anton Paar, Austria), water loss upon heating (140 °C), tapped (1000 automated cycles of compacting the powder by tapping glass cylinder with granulate and measuring weight and volume) and apparent density (free falling of granulate through funnel to 1 cm^3 cup and measuring weight), Hausner ratio, flowability analysis (PFT Powder Flow Tester, Brookfield, Canada) and BET Specific Surface Area (SSA) (SA 3100 Surface Area Analyzer, Beckman Coulter, Germany) and particle size distribution (LS 13 320 Laser Diffraction Particle Size Analyzer, Beckman Coulter Inc. USA). Water dispersions of SiC, both used Si powders and C were subjected to Zeta Potential analysis (ZetaProbe 75 Analyzer, Colloidal Dynamics, LLC, USA). Refractive indexes, extinction coefficients, and dielectric constants, needed for analysis, were taken from Ref. [25] for SiC, Ref. [26] for Si, and Ref. [27] for C.

Sintered samples were examined by means of optical microscopy, SEM microscope (NOVA NANO SEM 200, FEI, Netherlands) equipped with EDS (EDAX, Germany) analyzer and XRD analysis using PANalitycal X-Ray Diffractor (Malvern Panalytical, United Kingdom). Sintered samples were subjected to optical microscopy observations using LEICA DM2500 M (LEICA, Germany) and microstructure characterization using SEM microscope (NOVA NANO SEM 200, FEI, Netherlands) equipped with EDS (EDAX, Germany) analyzer. Additionally, selected sample were analyzed by means of helium density using AccuPyc II 1340 (Micromeritics Instruments, USA).

3. Results

3.1. Spray drying

Fig. 1 presents SEM images of the used powders showing their basic morphology. It can be observed that all of the powders are characterized by rough, irregular shapes. It is known that flowability of powders is closely related to interparticle forces. Because of that, the particle shape is strongly determining the flow behavior of powder. The packing density of non-spherical particles will be reduced in comparison to spherical ones. This leads to increased distances between centers of the gravity of the particles, which as a consequence lowers its homogenous ability to free flow [17]. Because of the small particle size of used powders (less than 10 μm), attractive electrostatic, capillary and Van der Waals forces dominate. This is especially true for irregularly shaped rough powders. It was found that the more spherical and smoother surface of a particle, the lower Van der Waals forces are, which further decreases the uncontrolled agglomeration of such powders [28]. Table 2 contains analysis data for initial powders.

The high Hausner ratios given in Table 2 implement, that none of commercially available powders could be considered as passable flowable. As a solution, spray drying of SiC- based granulates was proposed and developed. The preparation of such materials requires careful optimization of the process parameters together with the initial composition of the ceramic slurry. It was prepared by mixing SiC and Si powder (with the optional C addition) with organic binders and distilled water in calculated proportions. Zeta potential measurements of the commercially available powders were necessary in order to define the pH range that allows for the co-dispersing of all the mixed particles – Fig. 2.

The data obtained from the analysis gives the basic information of pH in which SiC ceramics should be processed. In this case, the pH should be slightly acidic (range between 6 and 7). Additionally, it is clearly visible that the addition of C will lead to an increase of pH ($IEP_{SiC} \approx 4{,}85$, $IEP_{Si} \approx 0{,}90$, and $IEP_C \approx 8{,}05$). The high isoelectric point (IEP) of carbon was most likely caused by chemical groups introduced during preparation method. It was previously reported that production method of carbon powder can significantly increase the base IEP point of active carbon of about 5.48 [29]. This has to be taken into account since fine Si powder is prone to reaction with water in pH > 8.5 with an extensive H2 release. It can lead to ignition during spray drying due to given friction during atomization. As a result, pH control was necessary. The pH adjustments of the slurry were made using 10 vol% 0.1 molar NH_4OH (increasing pH) or 1 vol% 0.1 molar HCl/HNO_3 (decreasing pH) water solutions. After

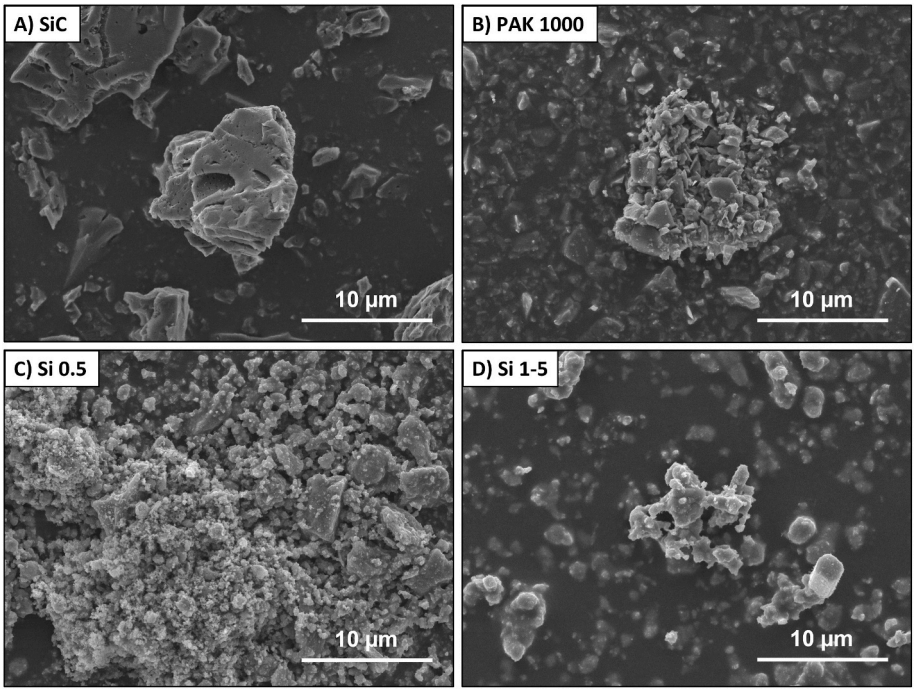

Fig. 1. SEM images of initial commercially available powders: A) SiC F2000; B) C PAK1000C) Si (0.5 μm); D) Si (1–5 μm).

Table 2
Initial powders' basic characterization data.

Powder	SSA [m^2/g]	ρ_{He} [g/cm^3]	ρ_{tap} [g/cm^3]	ρ_{app} [g/cm^3]	Hausner ratio
SiC F2000	4.67	3.30	0.92	0.61	1.51
Si (0.5 μm)	8.29	2.35	0.66	0.45	1.47
Si (1–5 μm)	0.98	2.37	1.08	0.58	1.86
C PAK1000	1050.43	2.39	0.50	0.33	1.52

SSA – Specific Surface Area.
ρ_{He} – Helium density.
ρ_{tap} – tapped density.
ρ_{app} – apparent density.

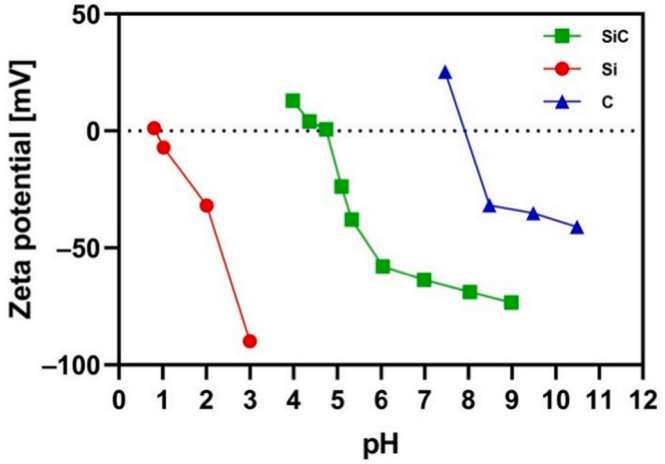

Fig. 2. Zeta potential of all 3 types of used powders - SiC, fine Si (0.5 μm), and C.

initial trials with both Si powders and C, it was observed that fine Si powder cannot be combined with C in the same slurry. Higher pH (caused by the introduction of C) led to an extensive reaction between Si and H_2O with the release of explosive hydrogen:

$$Si + H_2O \rightarrow SiO_2 + H_2\uparrow$$

Due to high Specific Surface Area (SSA) of the fine Si pH adjustment was not successful. Introduced Cl^- and NO_3^- ions promote corrosion of Si in water which contradicts the pH reduction effect. On the contrary, it was easy to modify the pH of mixtures with coarser Si powder. Polyvinyl alcohol (PVA) was selected as a binder in the form of 10 wt% water solution.

Another carbon source was proposed in form of spherical latex in order to prevent increase in pH of slurries. It was introduced to the system in form of fine spheres (d_{latex} = 450 nm) as a 50 wt% water dispersion. The amount of residual carbon originating from latex was calculated based on the conducted pyrolysis of a known amount of SiC-based granulate and latex for 4 h at 800 °C in an air atmosphere using a tube furnace. It allowed to determine the amount needed for a stoichiometric reaction between carbon and Si addition in granulate.

Optimization of the spray drying parameters guaranteed the preparation of high-quality granulates with a spherical shape, single modal particle size distribution, and acceptable flowability. The final compositions of the used SiC-based slurries are collected in Table 3 below.

It was discovered that slurries containing coarser Si powder with more than 30 vol% of solid load (SiC and Si content combined) were difficult to process due to nozzle clogging. This could be due to a strongly increasing viscosity. However, the successful production of granulates with 35 vol% (S1) and 33 vol% solid load (L1) slurries was possible despite initial problems. The SiC to Si volume ratio in the produced granulates after spray drying was about 5 to 1. Optimized parameters for all granulates were as follows: inlet temperature = 150 °C,

feed rate = 7 ml/min, aspirator rate = 80%, air flow = 473 l/h.

Table 3
Composition of SiC-based slurries for spray drying.

ID[a]	Si powder	SiC content (vol%)	Si content (vol%)	C content (relation to Si)	PVA content (vol% of solid load)	Water content (vol%)
S1	0.5	30	5	–	5	balance
S2	1–5	25	5	–	5	balance
C1	1–5	25	5	0.95	5	balance
L1	0.5	27	6	0.97	3	balance
L2	0.5	25	5	0.97	3	balance
L3	1–5	25	5	0.97	3	balance

[a] Where *S – Si; C – Si and C; L – latex and Si.*

3.2. Granulates characterization

The produced granulates were analyzed by means of particle size distribution, tapped and apparent density, flowability (rheological analysis), and H_2O content. The results are collected in Table 4.

All of produced granulates have a Hausner ratio which is considered passable for laser processing. It is especially true for granulates with latex (L1, L2, L3) with low values between 1.13 and 1.19. This confirms that spray drying is a suitable method for manufacturing SiC-based granulates, which have a fair flowability (Hausner ratio <1.25) and contain the addition of Si and C particles to enable a reactive laser sintering and liquid phase favorable for consolidation. The morphology of prepared materials is shown in Fig. 3.

It can be observed that S1, S2 and C1 granulates are characterized by the presence of rough particles on the surface. It is directly connected to the shape of the commercially available powders used for the preparation of the ceramic slurry. On the contrary, granulates produced with latex addition have a smooth surface. It occurred as a result of filling

Table 4
Analysis data of spray-dried granulates.

ID[a] (Si particle size in μm)	d_{10} [μm]	d_{50} [μm]	d_{90} [μm]	ρ_{tap} [g/cm^3]	ρ_{app} [g/cm^3]	Hausner ratio	H_2O content [%]
S1 (0.5)	6.79	15.98	32.48	0.87	0.66	1.31	0.71
S2 (1–5)	6.98	16.22	33.28	0.92	0.71	1.30	0.41
C1 (1–5)	7.07	17.17	39.47	0.92	0.72	1.27	0.35
L1 (0.5)	7.23	15.93	34.20	0.94	0.80	1.17	0.47
L2 (0.5)	6.23	13.93	29.19	0.91	0.76	1.19	0.63
L3 (1–5)	6.23	13.78	29.14	0.94	0.83	1.13	0.37

d_{10}, d_{50}, d_{90} – particle diameter of granulate.
ρ_{tap} – tapped density.
ρ_{app} – apparent density.
[a] Where *S* – Si; *C* – Si and C; *L* – latex and Si.

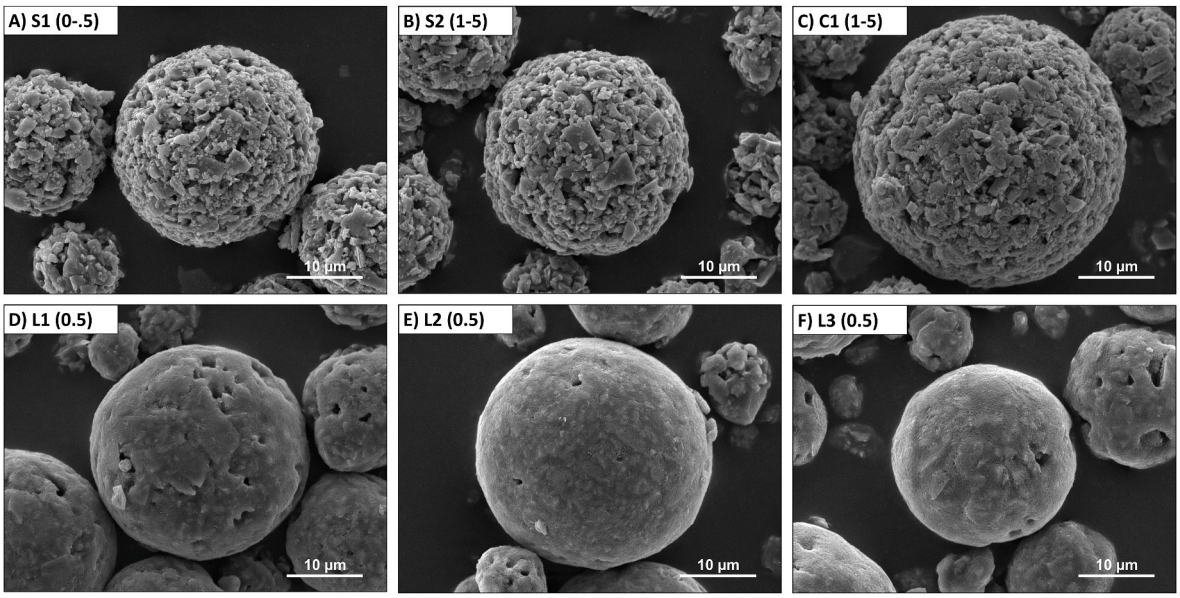

Fig. 3. SEM images of the morphology of SiC-based granulates.

gaps between SiC and Si particles by the fine latex spheres as visible in Fig. 4A and B. The differences are also reflected in the Hauser ratio measurements (Table 4). The values are significantly smaller for granulates with latex addition. Furthermore, granulates were inserted into a resin (Duracryl Plus, Spofa Dental, Czech Republic) and mechanically polished (down to 1 µm diamond dispersion) in order to reveal the inner morphology of the granulates. A representative image is shown in Fig. 4C. It can be seen that roughly shaped SiC particles are closely packed inside the granule. No internal defects such as cracks or hollow cores were observed in any of the six produced granulates.

Rheological analysis results are collected in Fig. 5. The measurement was conducted according to the numerical Jenik classification [26] based on the flow function *ff* which is the ratio of the major principal consolidation stress $\sigma 1$ and the unconfined failure strength σc. By superimposing simply defined flow onto flow function diagrams, it is possible to directly assign the investigated granules to one of five flow types: non-flowing, very cohesive, cohesive, easily flowing, free flowing, corresponding to the behavior of the granules during flow. The recorded flow functions classify all the tested granules as easy flowing ($4 < ff < 10$) as can be seen in Fig. 5A. The best characteristic was recorded for granule L1, whose flow function in the consolidation stress range up to 10 kPa lays on the easy flowing/free flowing field separation line ($ff = 4$). The lowest values of the consolidation ratio were recorded for granules L2 and L3, but the recorded curves are still in the middle of the easy flowing field. Overall, all granules flowed very well and there was little difference between them. The measured changes in bulk density (Fig. 5B) confirm the relatively small differences between the rheological properties of the tested granules - the recorded increases are proportional for all of them. Noticeably higher bulk density values were recorded for granules L1-L3 than for the other granules. For this measurement, the poorer rheological properties become apparent in the form of a faster increase in bulk density as a function of consolidation stress. For the investigated granules, the recorded increments are comparable. Measurements of the effective angle wall friction (Fig. 5C) and effective angle internal friction (Fig. 5D) divided the tested granules into two groups - L1-L3, for which the smallest values were recorded, and the others C1, S1, S2, for which slightly smaller values were recorded. It confirms that latex addition allowed for improvement of flowability. It is especially true for granulate L1 for which recorded values of effective angle wall friction and effective angle internal friction were the smallest.

3.3. Selective laser sintering

Laser sintering was used for the direct production of RBSiC by a single step method. The main advantage of this method is one step sintering process. Laser beam locally delivers energy in form of the electromagnetic wave to the material surface, in order to sinter small part of ceramic powders at once. Adjustment of different process parameters can be used to produce porous, dense, or gradient structures with shaping freedom. Processing was conducted by two techniques, producing varying results. The first one uses a granulate/isopropyl alcohol dispersion (30/70 vol%) to spray deposit granulates on a hot pressed SiC substrate - layer thickness of about 80 µm. The second method employed granulates pressed into circular green samples: d =

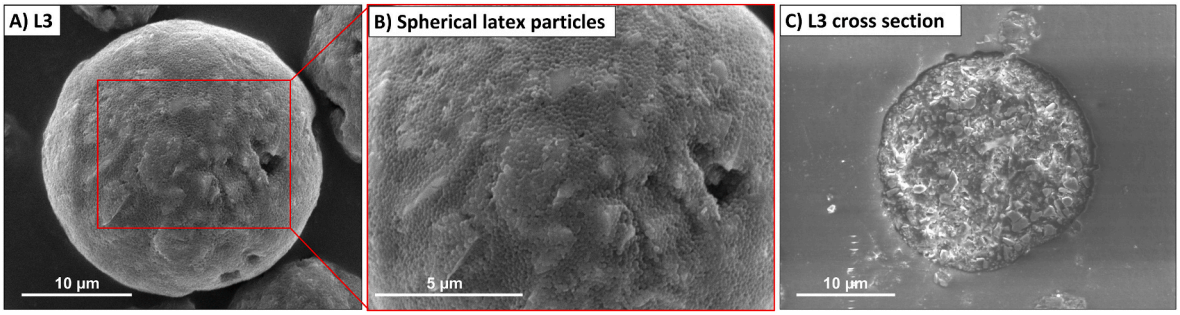

Fig. 4. SEM image of L3 (0.5) granule, B) spherical latex particle on the surface of L3 granule, C) L3 granule cross-section.

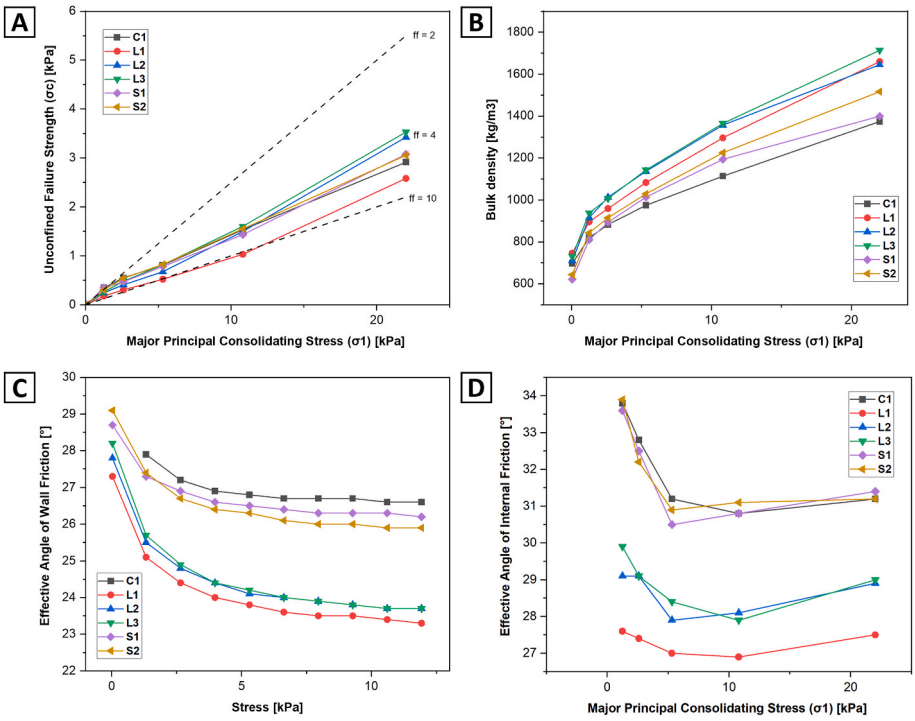

Fig. 5. Rheology of SiC granulates A) Unconfined Failure Strength, B) Bulk density, C) Effective Angle of Wall Friction, D) Effective Angle of Internal Friction.

25 mm, h = 3 mm, p = 10 MPa. Both types of prepared samples were put into the isolated reaction chamber. It was filled with N_2 to an over-pressure of 1 atmosphere in order to prevent excessive oxidation during laser processing. A schematic representation of the laser apparatus setup is presented in Fig. 6. The processing of samples was conducted using a fiber Nd:YAG laser with a wavelength of 1064 ± 10 μm. The laser scanner head equipped with an optical mirror system allowed for precise control of laser beam movement.

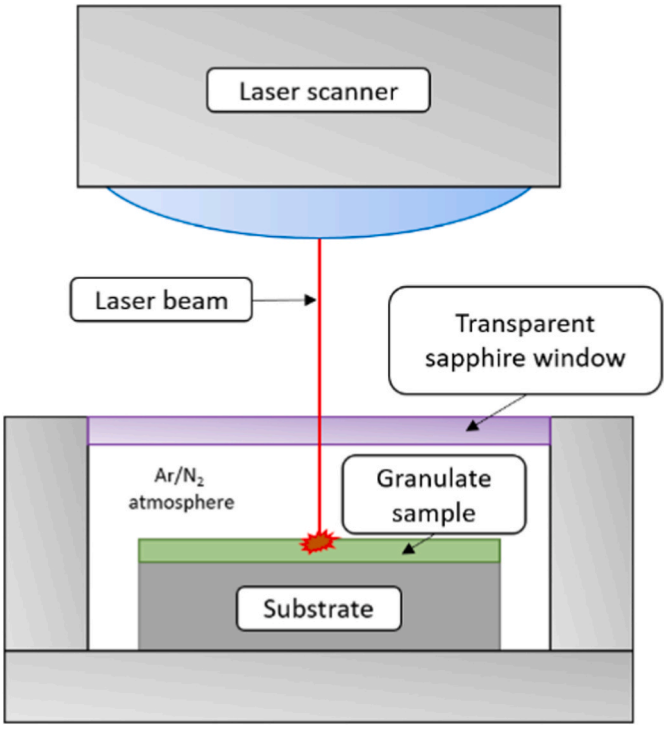

Fig. 6. Schematic representation of laser apparatus.

Based on experimental trials, the processing parameters were adjusted in order to produce crack-free material with no delamination between layers and are shown in Table 5. It was observed that depending on the sample preparation method, different laser working modes were more beneficial for processing. Single Sector Pulse mode with a small diameter of the laser beam was used for spray-deposited samples. On the contrary, the continuous work mode was more beneficial for pressed samples that are characterized by higher density than the spray-deposited samples. It was necessary to significantly lower the power density by increasing beam diameter because of an occurring material decomposition during continuous laser processing.

As can be seen in Fig. 7, the decomposition of the SiC granulates of the L1 (0.5) composition can be observed in form of brighter areas around the parts subjected to increased laser power. It was caused by the evaporation of silicon during high-energy processing. It was determined that too fast scanning speed did not allow for sufficient energy absorption from laser beam necessary for temperature increase that stimulates reactive sintering of granulate. Additionally, it is visible that laser power of 30 W and more, resulted in delamination of laser treated granulate from the substrate. On the contrary, laser power of 5 and 10 W did not provide enough energy for proper sintering – it was found later that material is breaking apart during cleaning. After removal of excess granulate followed by SEM observations, it was determined that area marked on Fig. 7 is characterized by the most homogenous microstructure.

Table 5
Laser processing parameters.

Sample preparation route	Spray deposited	Pressed green sample
Working mode	Single Sector Pulse	Continuous
Laser beam diameter [μm]	40	200
Track spacing [mm]	0.01	0.01
Scanning speed [m/s]	0.05	0.025
Power [W]	20	20
Max power density [W/cm^2]	3.18e+6	1.27e+5
Frequency [kHz]	20	–
Pulse duration [μs]	10	–

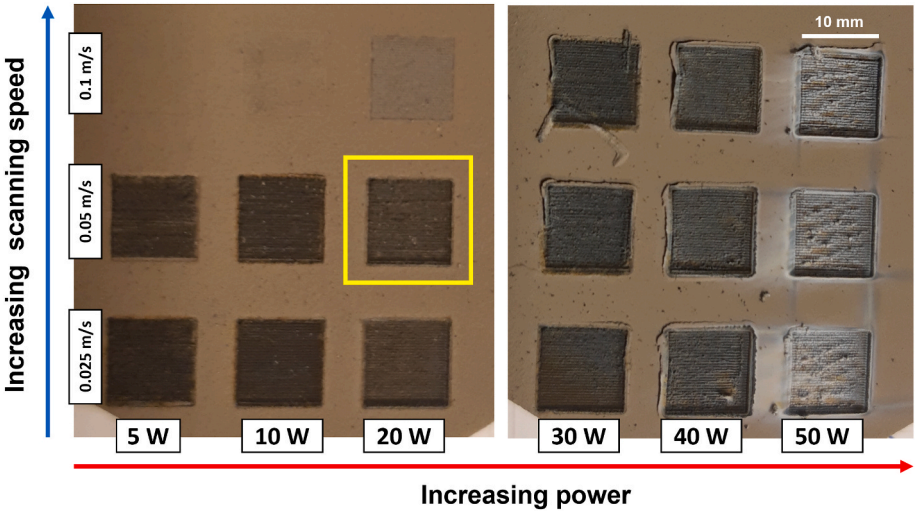

Fig. 7. Effect of changed parameters on L1 SiC granulate deposited on bulk SiC ceramic substrate – high power led to extensive decomposition of material and recrystallization of Si and SiO_2 on the surface (white areas on the left).

Because of that, it was selected for element mapping performed by the SEM-EDS technique on the granulate-substrate boundary as shown in Fig. 8. The differences between SiC substrate and laser-treated SiC granulates are easily noticed. The latter is characterized by a porous structure, with visible granulate particles sintered together (higher magnifications in Fig. 10), while hot pressed SiC substrate shows presence of elongated needle-like grains that formed during prolonged high temperature exposure under high pressure conditions. The marked boundary area is slightly enriched with oxygen – which was most likely absorbed on the particle surface during spray drying and then reacted with SiC-based material during laser action. It shows higher concentration in this area because of lack of repetitive laser beam action, which induces removal of excess oxygen, in comparison to material in the center of processed shape. Similarly, carbon depletion in the same area is caused by SiC decomposition during which Si and C reacts with oxygen and form SiO_2 and CO_2 respectively.

Observations performed by optical microscopy on laser-sintered SiC green samples, shows that a power of 20 W and a laser beam diameter of 200 μm lead to satisfactory result (Fig. 9A). An increased power led to an excessive formation of cracks between the laser scanning tracks (Fig. 9B). Additionally, it was observed that a higher laser power resulted in decomposition of SiC which can be observed as an increased bright gray area on the sample surface. Due to these observations, the sample obtained from the L1 (0.5) SiC granulates with a power of 20 W was selected as the one for further investigation.

SEM analysis of the same samples allowed to measure the depth of laser treatment inside the pressed granulates. It was confirmed that the depth of sintering reached about 75 μm (Fig. 10A). Observations of the sintered surface revealed a porous uniform microstructure with no visible cracks (Fig. 10B). Sintered granulate maintained their initial

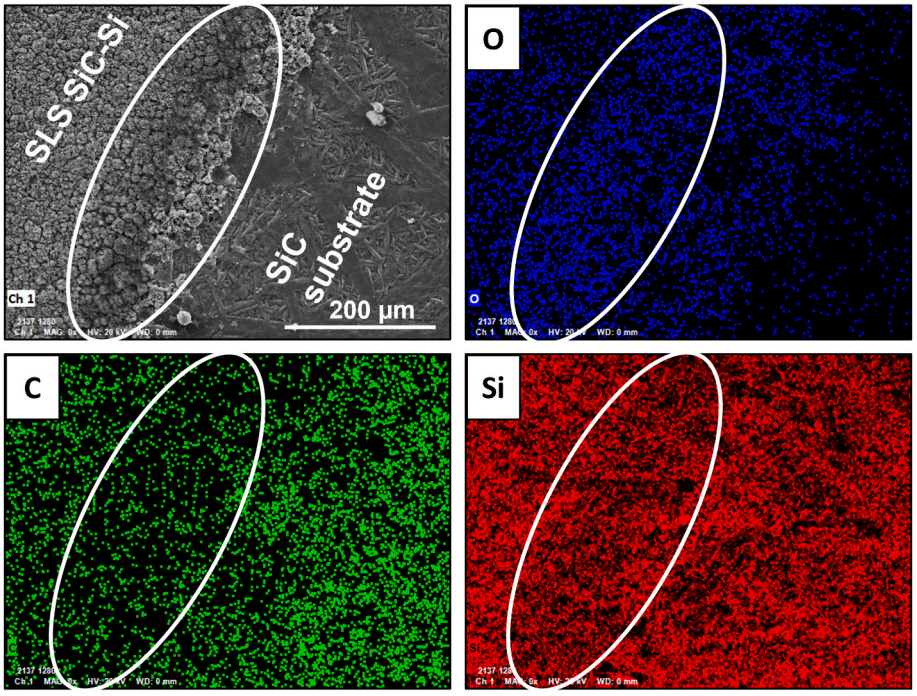

Fig. 8. SEM EDS map analysis of sintered spray deposited L1 granulate on SiC substrate – best quality of the sintered sample is marked; B) SEM element maps of the area with sintered granulates and substrate.

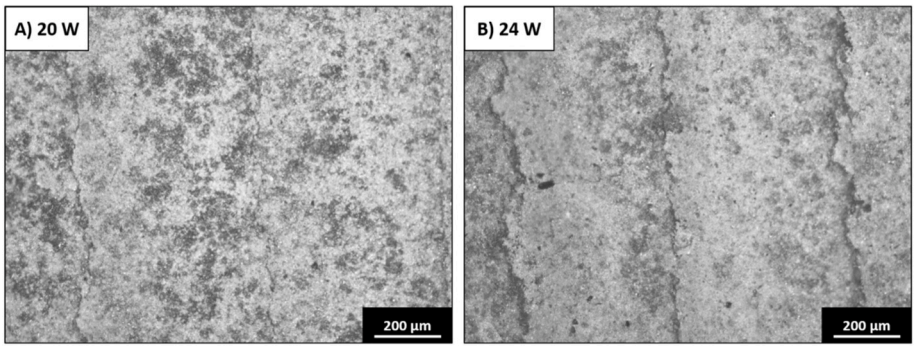

Fig. 9. Optical microscope images of surface of laser-treated L1 SiC granulates pressed into green samples – more power caused excessive cracking of the material.

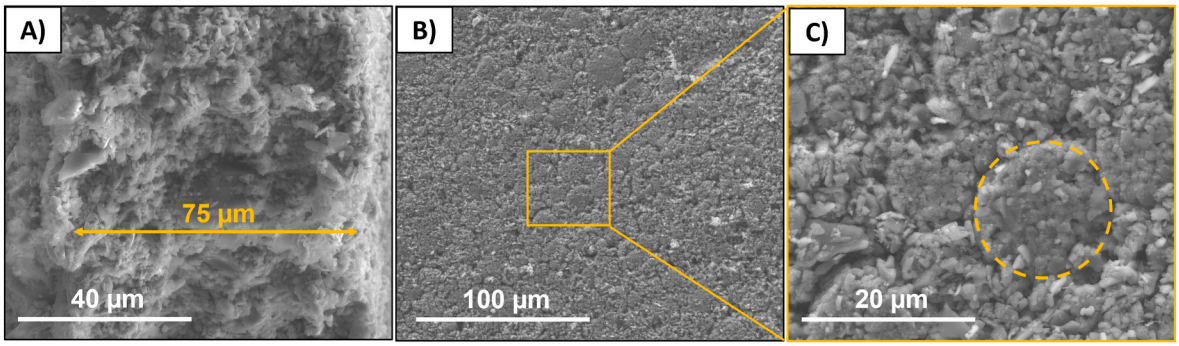

Fig. 10. SEM images of laser-treated L1 SiC granulates: A) fracture – depth of sintered material reaches about 75 µm; B) and C) surface–sintered particles of granulate can be observed.

shape and can be observed in Fig. 10B and C. Their sizes are similar to previously measured granulate particles (15–20 µm). Laser action led to the decomposition of latex particles previously visible on the granulates surface.

In order to check the phase composition of the sintered samples, XRD analysis was carried out on a sample obtained from the L1 (0.5) granulate using 20 W laser power, that possessed the best microstructure (Fig. 10). The results (Fig. 11) confirmed that most of the material was SiC (96.2%). Some residual Si (2.4%) and C (1.4%) were present in the material after laser treatment, but it was most likely located at the surface. When compared to the initial amount of Si in this granulate The final amount of SiC shows that a reaction between additionally introduced Si and C occurred during laser action. The SiO_2 was not detected by XRD – the amount of formed SiO_2 phase was too low to be detected by the XRD method. Additionally, it could possess an amorphous structure which makes it even more difficult to detect in such small amounts. Selected sample obtained from pressed granulate (granulate L1) was analyzed by means of helium density. The calculated average value of relative density after 5 measurements was 41.62 ± 9.53%. This is lower than the results obtained in similar studies using polymer preforms manufactured by laser processing which were processed further to obtain SiC structures [30].

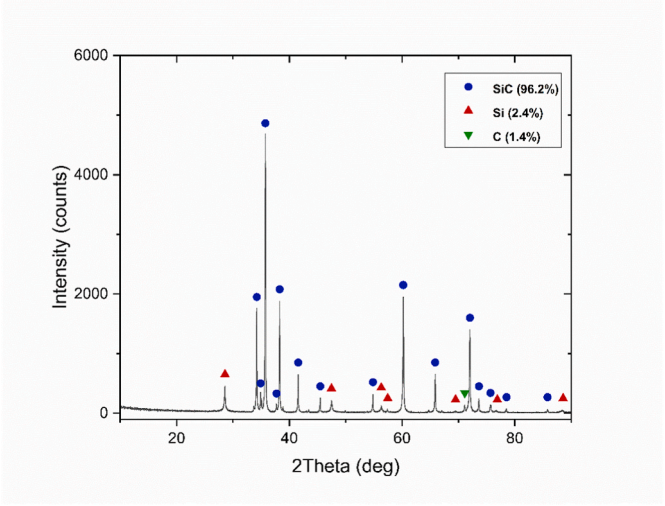

Fig. 11. XRD pattern of laser-sintered L1 (0.5) SiC granulate.

4. Discussion

The preparation of slurry with pure carbon was problematic due to a drastic increase in pH, which led to the reaction of Si with water releasing hydrogen that could explode during spray drying. This was solved by replacing carbon powder with latex in form of 50/50 wt% water dispersion as a carbon source. It had an additional effect of smoothening granules' surface, which was beneficial for flowability. The organic carbon sources are widely known as a possible solution while sintering RBSiC either as gas [31] or liquid/solid sintering aid [32].

Previous research states that the design and production of granulates have to meet a collection of different parameters to make granulates suitable for Additive Manufacturing processes [17,33]. However, two main principles had been agreed on: the spherical and large granules exhibit better flow behavior than small and rough particles [34,35], maximum packing of powders can occur when the size ratio of coarse/fine particles is higher than 1:10 while there is at least about 70 vol % of coarse particles [36,37]. Based on that, the Hausner ratio and rheological analysis of the prepared granulates show very promising results and are defined as, at least, easy flowable or better. Modification of granulate composition was possible in terms of the introduction of Si as an additional sintering aid that can react with C in order to directly

produce Reaction Bonded SiC during laser processing. Similar ideas were successfully employed using Direct Laser Sintering [12] and the Silicon infiltration method [14]. However, above mentioned experiments, needed at least two technological steps: preparation of preform and gas infiltration/pyrolysis reaction, in order to produce RBSiC. The approach presented in this study shows that Laser Processing of RBSiC can be done in one step. Additionally, the SiC/Si/latex granulate production method can be scaled up to industrial quantities relatively easily, because of the used spray drying technique, which is widely known and used in many different branches (not only the ceramic industry).

The laser treatment was conducted using two approaches. The first one showed that spray-deposited SiC granulates on hot-pressed SiC can be sintered by the use of a small diameter of the laser beam operating with very short and high-energy pulses. Because of the rapid laser action, it was difficult to properly control the process which led to the decomposition of the material exposed to the high-energy laser beam. Therefore, a different approach was proposed. Granulate pressed into a green sample was subjected to a continuous work laser treatment. It allowed for a better control of the process parameters because of a much lower energy density.

The L1 (0.5) granulate processed with a laser power of 20 W was selected for further investigation. Optical microscope and SEM observations confirmed the uniformity of the material. The morphology of the sintered layers was highly porous. XRD analysis confirmed that most of the Si reacted with C to SiC originating from both PVA binder and latex. No SiO_2 was detected in the sample. The calculated relative density of sinter proves that SLS of granulate manufactured by spray drying can be laser processed in order to obtain porous SiC. Based on that it can be stated that RBSiC was successfully obtained in a single step process.

5. Conclusions

Conducted experiments lead to the following conclusions:

- Spray drying can be successfully used as a production method of SiC-based granulates with significantly improved flowability in comparison to commercially available powders
- The explosion hazard of using fine active carbon in combination with pure silicon in water-based ceramic slurries has to be considered. This follows due to a significant shift to an acidic pH value leading to the reaction between silicon and water with the release of explosive hydrogen
- The addition of latex as an alternative carbon source for reaction with silicon was beneficial for the flowability of obtained granulates, it also allowed for the reaction between Si and C during laser sintering resulting in RBSiC
- It is possible to use spray-dried SiC-based granulates for a successful laser sintering after appropriate optimization of the granulation process
- It is possible to upscale spray drying for industrial quantities because of its popularity in many different industries
- The laser-sintered material possessed porous morphology with no cracks observed
- XRD analysis confirmed that most of the introduced silicon and carbon reacted with each other, thus a direct reaction bonding of SiC was successfully performed in a single step approach via selective laser sintering
- SLS of granulate obtained by spray drying can be successfully used to sinter porous SiC

Because it was confirmed that granulates possess good flowability and a composition that allows a direct reaction bonding during laser sintering, further investigation on larger-scale structures is planned using other laser systems. This will allow for mechanical testing of obtained material as well as porosity measurements. Further investigations will also aim to directly produce porous SiC filters (sterile water filters) containing a gradient structure with pore sizes down to 300 nm using the spray-dried granulates and selective laser sintering.

Declaration of competing interest

The authors declare the following financial interests/personal relationships which may be considered as potential competing interests: Jan Huebner reports financial support was provided by Swiss National Science Foundation.

Acknowledgment

This research was supported by the Swiss National Science Foundation [grant number IZSEZ0_201435, „Reactive laser sintering of silicon-based ceramics (ReLaSiC)"].

References

[1] K. Biswas, Solid state sintering of sic-ceramics, Mater. Sci. Forum 624 (2009) 71–89. https://doi.org/10.4028/www.scientific.net/MSF.624.71.
[2] Y. Wang, S. Dong, X. Li, C. Hong, X. Zhang, Synthesis, properties, and multifarious applications of SiC nanoparticles: a review, Ceram. Int. 48 (2022) 8882–8913, https://doi.org/10.1016/j.ceramint.2021.12.208.
[3] T. Koyanagi, K. Terrani, S. Harrison, J. Liu, Y. Katoh, Additive manufacturing of silicon carbide for nuclear applications, J. Nucl. Mater. 543 (2021), 152577, https://doi.org/10.1016/j.jnucmat.2020.152577.
[4] R.J. Lewis, Sax's Dangerous Properties of Industrial Materials, eighth ed., Van Nostrand Reinhold, 1990.
[5] A. Saleem, Y. Zhang, H. Gong, M.K. Majeed, Fluoride doped SiC/Si3N4 composite as a high thermal conductive material with enhanced mechanical properties, Ceram. Int. 45 (2019) 21004–21010, https://doi.org/10.1016/j.ceramint.2019.06.289.
[6] S. Shahrestani, M.C. Ismail, S. Kakooei, M. Beheshti, Effect of additives on slip casting rheology, microstructure and mechanical properties of Si3N4/SiC composites, Ceram. Int. 46 (2020) 6182–6190, https://doi.org/10.1016/j.ceramint.2019.11.085.
[7] Q. Liu, F. Ye, Z. Hou, S. Liu, Y. Gao, H. Zhang, A new approach for the net-shape fabrication of porous Si3N4 bonded SiC ceramics with high strength, J. Eur. Ceram. Soc. 33 (2013) 2421–2427, https://doi.org/10.1016/j.jeurceramsoc.2013.04.034.
[8] X. Li, Y. Nakata, H. Nagai, M. Suzuki, Synthesis and thermal stability of SiC-Si3N4 composite ultrafine particles by laser-induced gas-phase reaction, Nanostruct. Mater. 10 (1998) 1173–1187, https://doi.org/10.1016/S0965-9773(98)00147-0.
[9] M. Li, L. Cheng, R. Mo, F. Ye, X. Yin, (SiC-Si3N4)w/SiBCN composite ceramics with tunable electromagnetic properties, J. Alloys Compd. 798 (2019) 280–289, https://doi.org/10.1016/j.jallcom.2019.05.192.
[10] C. Chen, X. Liang, M. Luo, S. Zhou, J. Ji, Z. Huang, M. Xu, Preparation and characterization of porous Si3N4-bonded SiC ceramics and morphology change mechanism of Si3N4 whiskers, Ceram. Int. 45 (2019) 5922–5926, https://doi.org/10.1016/j.ceramint.2018.12.060.
[11] H. Ghanem, H. Gerhard, N. Popovska, Paper derived SiC-Si3N4 ceramics for high temperature applications, Ceram. Int. 35 (2009) 1021–1026, https://doi.org/10.1016/j.ceramint.2008.04.020.
[12] S. Meyers, L. De Leersnijder, J. Vleugels, J.P. Kruth, Direct laser sintering of reaction bonded silicon carbide with low residual silicon content, J. Eur. Ceram. Soc. 38 (2018) 3709–3717, https://doi.org/10.1016/j.jeurceramsoc.2018.04.055.
[13] P. Ge, Y. Cheng, K. Sun, Structure and performance of Si 3 N 4/SiC/CNT composite fibres, Ceram. Int. 45 (2019) 12677–12681, https://doi.org/10.1016/j.ceramint.2019.03.099.
[14] P.S. Grinchuk, M.V. Kiyashko, H.M. Abuhimd, M.S. Alshahrani, M.O. Stepkin, V. V. Toropov, A.A. Khort, D.V. Solovei, A.V. Akulich, M.D. Shashkov, M.Y. Liakh, Effect of technological parameters on densification of reaction bonded Si/SiC ceramics, J. Eur. Ceram. Soc. 38 (2018) 4815–4823, https://doi.org/10.1016/j.jeurceramsoc.2018.07.014.
[15] X. Liu, X. Yin, W. Duan, F. Ye, X. Li, Electromagnetic interference shielding properties of polymer derived SiC-Si3N4 composite ceramics, J. Mater. Sci. Technol. 35 (2019) 2832–2839, https://doi.org/10.1016/j.jmst.2019.07.006.
[16] D. Li, E. Guzi De Moraes, P. Colombo, Z. Shen, Preparation of nasal cavity-like SiC-Si3N4 foams with a hierarchical pore architecture, RSC Adv. 5 (2015) 27891–27900, https://doi.org/10.1039/c5ra00766f.
[17] A.B. Spierings, M. Voegtlin, T. Bauer, K. Wegener, Powder flowability characterisation methodology for powder-bed-based metal additive manufacturing, Prog. Addit. Manuf. 1 (2016) 9–20, https://doi.org/10.1007/s40964-015-0001-4.
[18] A.B. Yu, J.S. Hall, Packing of fine powders subjected to tapping, Powder Technol. 78 (1994) 247–256, https://doi.org/10.1016/0032-5910(93)02790-H.
[19] M.A. Kaleem, M.Z. Alam, M. Khan, S.H.I. Jaffery, B. Rashid, An experimental investigation on accuracy of Hausner Ratio and Carr Index of powders in additive manufacturing processes, Met. Powder Rep. 76 (2021), https://doi.org/10.1016/j.mprp.2020.06.061. S50–S54.

[20] M. Makowska, S. Pfeiffer, N. Casati, K. Florio, M. Vetterli, K. Wegener, T. Graule, H. van Swygenhoven, Pre-processing of hematite-doped alumina granules for selective laser melting, Ceram. Int. 45 (2019) 17014–17022, https://doi.org/10.1016/j.ceramint.2019.05.251.
[21] S. Pfeiffer, M. Makowska, K. Florio, D.F. Sanchez, F. Marone, X. Zhang, C. G. Aneziris, H. Van Swygenhoven, K. Wegener, T. Graule, Selective laser melting of thermal pre-treated metal oxide doped aluminum oxide granules, Open Ceram 2 (2020), 100007, https://doi.org/10.1016/j.oceram.2020.100007.
[22] X. Zhang, S. Pfeiffer, P. Rutkowski, M. Makowska, D. Kata, J. Yang, T. Graule, Laser cladding of manganese oxide doped aluminum oxide granules on titanium alloy for biomedical applications, Appl. Surf. Sci. 520 (2020), https://doi.org/10.1016/j.apsusc.2020.146304.
[23] S. Pfeiffer, K. Florio, M. Makowska, F. Marone, S. Yüzbasi, C.G. Aneziris, H. Van Swygenhoven, K. Wegener, T. Graule, Crack-reduced alumina/aluminum titanate composites additive manufactured by laser powder bed fusion of black TiO2−x doped alumina granules, J. Eur. Ceram. Soc. 42 (2022) 3515–3529, https://doi.org/10.1016/j.jeurceramsoc.2022.02.046.
[24] H. Lee, C.H.J. Lim, M.J. Low, N. Tham, V.M. Murukeshan, Y.J. Kim, Lasers in additive manufacturing: a review, Int. J. Precis. Eng. Manuf. - Green Technol. 4 (2017) 307–322, https://doi.org/10.1007/s40684-017-0037-7.
[25] J.I. Larruquert, A.P. Pérez-Marín, S. García-Cortés, L. Rodríguez-de Marcos, J. A. Aznárez, J.A. Méndez, Self-consistent optical constants of SiC thin films, J. Opt. Soc. Am. A 28 (2011) 2340, https://doi.org/10.1364/josaa.28.002340.
[26] S.E. Baroni, Peacemaking in international conflict: methods and techniques, Peace Change 35 (2010) 531–533, https://doi.org/10.1111/j.1468-0130.2010.00653.x.
[27] H.R. Phillip, E.A. Taft, Kramers-kronig analysis of reflectance data for diamond, Phys. Rev. 136 (1964), https://doi.org/10.1103/PhysRev.136.A1445.
[28] A. Castellanos, The relationship between attractive interparticle forces and bulk behaviour in dry and uncharged fine powders. https://doi.org/10.1080/17461390500402657, 2005.
[29] M.R. McPhail, J.A. Sells, Z. He, C.C. Chusuei, Charging nanowalls: adjusting the carbon nanotube isoelectric point via surface functionalization, J. Phys. Chem. C 113 (2009) 14102–14109, https://doi.org/10.1021/jp901439g.
[30] M. Pelanconi, P. Colombo, A. Ortona, Additive manufacturing of silicon carbide by selective laser sintering of PA12 powders and polymer infiltration and pyrolysis, J. Eur. Ceram. Soc. 41 (2021) 5056–5065, https://doi.org/10.1016/j.jeurceramsoc.2021.04.014.
[31] B.R. Birmingham, H.L. Marcus, Solid freeform fabrication of silicon carbide shapes by selective laser reaction sintering (SLRS), Proc. Solid Free. Fabr. Symp. (1995) 308–316.
[32] B.W. Xiong, H. Yu, Z.F. Xu, Q.S. Yan, Y.H. Zheng, P.L. Zhu, S.N. Chen, Study on dual binders for fabricating SiC particulate preforms using selective laser sintering, Composites, Part B 48 (2013) 129–133, https://doi.org/10.1016/j.compositesb.2012.09.092.
[33] M. Krantz, H. Zhang, J. Zhu, Characterization of powder flow: static and dynamic testing, Powder Technol. 194 (2009) 239–245, https://doi.org/10.1016/j.powtec.2009.05.001.
[34] X. Fu, D. Huck, L. Makein, B. Armstrong, U. Willen, T. Freeman, Effect of particle shape and size on flow properties of lactose powders, Particuology 10 (2012) 203–208, https://doi.org/10.1016/j.partic.2011.11.003.
[35] H. Lu, X. Guo, Y. Liu, X. Gong, Effect of particle size on flow mode and flow characteristics of pulverized coal, KONA Powder Part. J. 32 (2015) 143–153, https://doi.org/10.14356/kona.2015002.
[36] G. Egger, P.E. Gygax, R. Glardon, N.P. Karapatis, Optimization of powder layer density in selective laser sintering, 10th Solid Free, Fabr. Symp. (1999) 255–263. http://infoscience.epfl.ch/record/153069.
[37] D. Sofia, R. Chirone, P. Lettieri, D. Barletta, M. Poletto, Selective laser sintering of ceramic powders with bimodal particle size distribution, Chem. Eng. Res. Des. 136 (2018) 536–547, https://doi.org/10.1016/j.cherd.2018.06.008.